

Power insensitive silicon microring resonators

Lian-Wee Luo,^{1,*} Gustavo S. Wiederhecker,^{1,3} Kyle Preston,¹ and Michal Lipson^{1,2}

¹*School of Electrical and Computer Engineering, Cornell University, Ithaca, New York 14853, USA*

²*Kavli Institute at Cornell for Nanoscale Science, Cornell University, Ithaca, New York 14853, USA*

³*Current address: Instituto de Física Gleb Wataghin, Universidade Estadual de Campinas, CEP 13083-970, Campinas, Sao Paulo, Brazil*

*Corresponding author: ll399@cornell.edu

Received October 26, 2011; revised December 22, 2011; accepted December 22, 2011;
posted December 23, 2011 (Doc. ID 157110); published February 9, 2012

We demonstrate power insensitive silicon microring resonators without the need for active feedback control. The passive control of the resonance is achieved by utilizing the compensation of two counteracting processes, free carrier dispersion blueshift and thermo-optic redshift. In the fabricated devices, the resonant wavelength shifts less than one resonance linewidth for dropped power up to 335 μW , more than fivefold improvement in cavity energy handling capability compared to regular microrings. © 2012 Optical Society of America

OCIS codes: 190.1450, 230.5750.

Silicon microring resonators have revolutionized the field of silicon photonics for on-chip optical interconnects over the past decade. Optical interconnect networks utilizing silicon microring-based devices present a solution to the electrical interconnect bottleneck by offering a larger bandwidth, lower power consumption, and smaller device footprint in microelectronic chips [1–3]. However, silicon microresonators have one main drawback; that is, the resonant wavelength shifts with input optical power. At high powers, the stored light in a silicon microresonator is absorbed via two photon absorption (TPA) and generates free carriers. This results in a blueshift of the resonance owing to free carrier dispersion (FCD). In addition, the generated carriers lead to free carrier absorption (FCA). The TPA and FCA nonlinear processes, together with the linear surface absorption at the Si/SiO₂ interface, result in the heating of the resonator and cause a redshift in the resonance. In particular, reactive ion etching of the silicon induces surface and sidewall damage, resulting in the increased absorption sites at the Si/SiO₂ interface [4,5]. Etching also results in increased recombination sites and a shorter free carrier lifetime. Because of the dominant thermo-optic (TO) redshift over the FCD blueshift, an effective redshift of the resonance is observable in many etched silicon microresonators, such as microdisk, microring, and photonic crystal resonators [5–8].

The ability to tailor the microresonator spectral dependence on input power is critical. Several previous works to achieve microresonators with power-independent transmission spectra have been pursued. In one approach, polymer with a negative TO coefficient has been used as a cladding material to compensate for the positive TO microcavity [9,10]. But the use of polymers is not compatible with complementary metal-oxide semiconductor (CMOS) processes. Another work has utilized an additional stabilizing laser to compensate the TO effect, ensuring a Lorentzian line-shape transmission [11]; this approach is relatively power hungry. Here we demonstrate power insensitive silicon microring resonators using a passive technique by utilizing two counteracting processes, FCD blueshift

and TO redshift. It should be noted that this technique reduces the sensitivity dependence of the resonance on laser input power but not on ambient temperature.

To control the degree of spectral shift with optical power, we analyze the effective resonance shift $\Delta\lambda$ owing to the counteracting effects of FCD and TO processes in the silicon microresonator (neglecting the minor contribution of TO in the cladding SiO₂) [8,12]:

$$\Delta\lambda \approx \frac{\lambda_0}{n_g} (\Delta n_{\text{FC}} + \Delta n_{\text{T}}), \quad (1)$$

where λ_0 is the resonant wavelength, n_g is the group index of the microresonator, and Δn_{FC} and Δn_{T} are the refractive index changes of Si owing to the FCD and TO effects, respectively. The index change owing to FCD is expressed as $\Delta n_{\text{FC}} = -8.8 \times 10^{-22} \Delta N - 8.5 \times 10^{-18} (\Delta P)^{0.8}$, where ΔN and ΔP are the density of generated electrons and holes per cubic centimeter and $\Delta N = \Delta P = (\Gamma_{\text{FCD}} c^2 \beta / 2 \hbar \omega_0 n_g^2 V_{\text{FCD}}^2) \tau_{\text{FC}} U^2$. Γ_{FCD} is the effective confinement factor corresponding to FCD, c is the speed of light in free space, $\beta = 8.4 \times 10^{-22} \text{ m} \cdot \text{W}^{-1}$ is the TPA coefficient in silicon, \hbar is the reduced Planck constant, ω_0 is the resonant frequency of the resonator, V_{FCD} is the effective nonlinear mode volume, τ_{FC} is the free carrier lifetime, and U is the intracavity stored energy. The index shift owing to TO can be expressed as $\Delta n_{\text{T}} = \Gamma_{\text{th}} \left(\frac{dn_{\text{Si}}}{dT} \right) R_{\text{th}} \gamma_{\text{abs}} U$, where Γ_{th} is the effective confinement factor corresponding to the TO effect, $\frac{dn_{\text{Si}}}{dT} = 1.86 \times 10^{-4} \text{ K}^{-1}$ is the TO coefficient of silicon, R_{th} is the cavity thermal resistance, and γ_{abs} is the total cavity optical absorption rate (sum of linear absorption, TPA and FCA).

Equation (1) sets the guideline in designing the physical and geometrical properties of the resonator to balance the FCD blueshift and the TO redshift of the resonance. We can increase the FCD blueshift by designing a photonic structure with a long free carrier lifetime (τ_{FC}) to compensate the dominant TO redshift. We fabricate a 50 μm radius silicon microring resonator through selective oxidation using an etchless silicon fabrication

technique [13]. The dimensions of the microring are 800 nm wide by 60 nm high with a 6 nm thin slab and 1 μm coupling gap [14]. The silicon waveguide is not exposed to any etching plasma throughout the fabrication process, preventing damage from the ion bombardment and chemical reactions. This etchless technique results in an ultrasmooth Si/SiO₂ interface and reduces absorption and recombination sites.

We measure the free carrier lifetime of the fabricated etchless silicon microring resonator using a pump-probe optical setup [see Fig. 1(a)]. We couple into the microring an Er-fiber pulsed laser with 500 fs pulses, a 25 MHz repetition rate, and a spectral width of 6 nm at its center wavelength, $\lambda_{\text{pump}} = 1543$ nm. The pump pulses, with a peak power of 52 W, are absorbed by the silicon microring via TPA, and free carriers are generated. This results in a blueshift of the resonance owing to FCD. Concurrently, a quasi-TE polarized continuous-wave (CW) weak probe laser is coupled into the microring resonator and tuned to a near-linear portion of the resonance, $p_{\text{probe}} \approx 3$ μW and $\lambda_{\text{probe}} = 1489.484$ nm [see Fig. 1(b)]. The microring has a loaded quality factor $Q = 350,000$. The exponential growth in Fig. 1(c) is linearly related to the recombination of free carriers, and the experimental carrier lifetime is calculated to be 10 ns by fitting a simple exponential to the data. By avoiding reactive ion etching of the silicon, the effective τ_{FC} of the etchless silicon structure is more than 1 order of magnitude longer than that of an etched silicon microring [15].

Next we measure the microring power-dependent transmission using a CW tunable laser. In Fig. 2 we show the measured transmission (TE polarization) for several different CW laser power levels. At laser power of 10 μW , the microring is slightly undercoupled at 1542.162 nm. We observe that the resonance blueshifts with increasing input power, in contrast to the typical redshift in etched silicon microresonators. The effective blueshift is a result of the long free carrier lifetime of 10 ns. The net blueshift is large enough to induce optical bistability for power levels above 42 μW . Also, a reduction in the resonance extinction ratio and the optical quality factor is observed

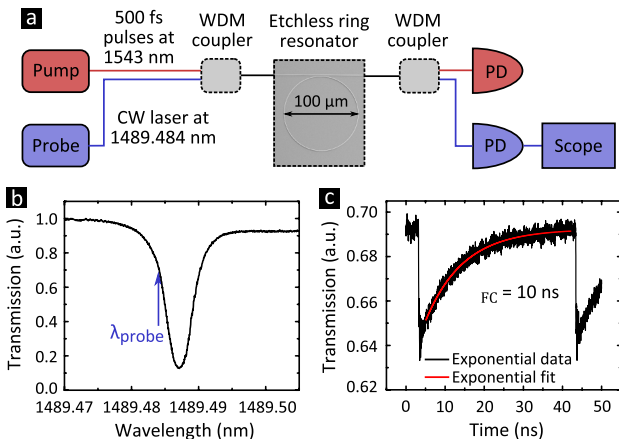


Fig. 1. (Color online) (a) Schematic diagram of the pump-probe setup for the measurement of free carrier lifetime. (b) Transmission spectrum of the etchless microring in quasi-TE polarization with $\lambda_{\text{probe}} = 1489.484$ nm. (c) Measurement of carrier lifetime.

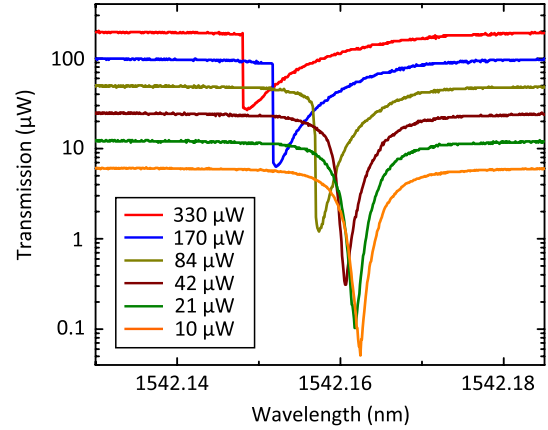


Fig. 2. (Color online) Measured transmitted power spectrum showing the net blueshift of the resonance with increasing laser input power (indicated in the inset). The laser is swept from longer wavelength to shorter wavelength.

owing to the increased nonlinear TPA and FCA losses. In this etchless microring, the FCD overcompensates the TO effect and becomes the dominant process, giving an effective blueshift of the resonance.

To control the resonance shift, we can engineer the thermal properties of the etchless silicon microring. In Fig. 3(a) we show the calculated resonant wavelength shift map of the etchless microring for a fixed τ_{FC} of 10 ns. To realize a power insensitive device, we etch trenches around the microring, as illustrated in Fig. 3(b), to increase the thermal resistance of the device ($R_{\text{th}} \approx 3000$ W/K). According to Fig. 3(a), such a value of R_{th} should result in a device with a very small power sensitivity. The thermal resistance can be controlled by varying the depth of the etched trenches, as shown in Fig. 3(c) [6]. The trenches are located 5 μm away from the guiding

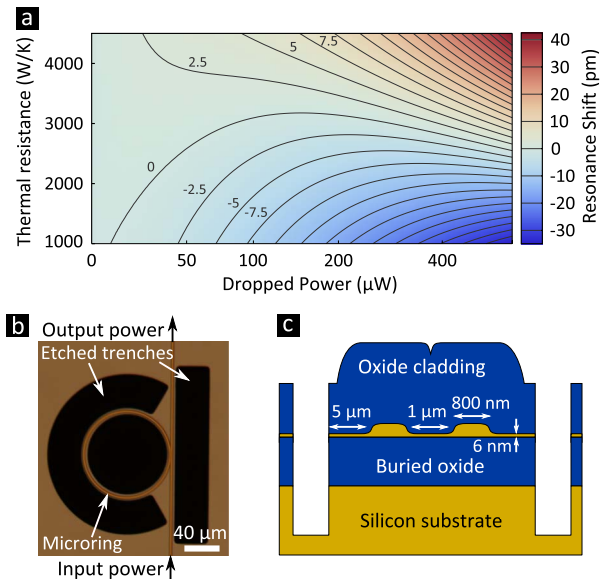


Fig. 3. (Color online) (a) Density plot calculating the resonance shift as a function of thermal resistance and dropped power. (b) Optical microscope picture of the fabricated etchless silicon microring resonator with etched trenches. (c) Schematic diagram of the cross section to illustrate the depth of the trenches (not drawn to scale).

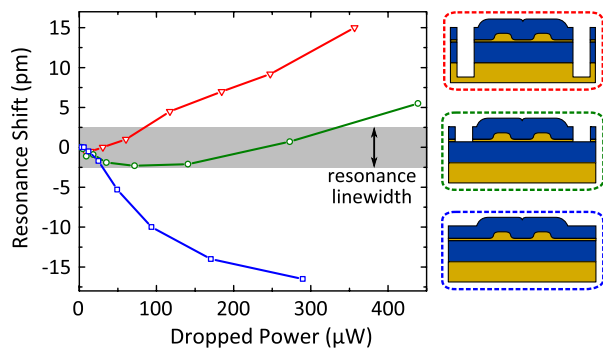


Fig. 4. (Color online) Measured resonance shift power dependence (at $\lambda_0 \approx 1542$ nm) of three different etchless silicon microring resonator devices: one without etched trenches (blue curve), one with just the silicon slab etched (green curve), and one with $300 \mu\text{m}$ deep trenches (red curve). The schematic insets on the right indicate the corresponding device cross section; the straight lines connecting the experimental data are guides for the eyes.

core, which prevents optical losses and degradation of carrier lifetime.

To analyze the effective resonance shift, we show in Fig. 4 the measured power-dependent wavelength shift of three etchless silicon microrings; each device with a different depth of the etched trenches. Each curve in Fig. 4 is obtained by extracting the minimum transmission wavelength ($\lambda_0 \approx 1542$ nm) for different power levels of the scanning CW laser, as in Fig. 2. In the resonator without trenches ($R_{\text{th}} = 1300$ K/W, blue curve in Fig. 4) there is a net blueshift, which becomes larger than one resonance linewidth at a dropped power around $30 \mu\text{W}$. By etching $300 \mu\text{m}$ deep trenches into the silicon substrate ($R_{\text{th}} = 3800$ K/W; see red curve in Fig. 4), there is a net redshift for dropped powers larger than $85 \mu\text{W}$. This shows that the trenches significantly increase the thermal resistance of the device and the TO effect becomes the dominant process. By etching away only the thin silicon slab ($R_{\text{th}} = 3000$ K/W; see green curve in Fig. 4), we obtain a power insensitive etchless silicon microring resonator for dropped power levels up to $335 \mu\text{W}$.

In conclusion, we demonstrate power insensitive silicon microring resonators by utilizing two counteracting processes, free carrier dispersion blueshift and thermo-optic redshift. In our fabricated devices, the resonant wavelength shifts less than one resonance linewidth for dropped power up to $335 \mu\text{W}$, and this represents a

fivefold improvement in cavity energy handling capability, as compared to a regular etched microring [7]. This compensation technique can also be employed in other resonator-based devices with a long carrier lifetime [16].

The authors thank M. Soltani and B. Guha for productive discussions. This work was supported in part by the Defense Advanced Research Projects Agency (DARPA) under the Zeno-based OptoElectronics program, the Army Research Development and Engineering Command (ARMYRDECOM) Award No. W911NF-11-1-0435 supervised by Dr. Jag Shah, and the National Science Foundation under Grant No. 1143893 and was performed in part at the Cornell NanoScale Facility, a member of the National Nanotechnology Infrastructure Network, which is supported by the NSF. Lian-Wee Luo acknowledges a fellowship from Agency of Science, Technology and Research (A*STAR), Singapore.

References

1. D. A. B. Miller, *IEEE J. Sel. Top. Quantum Electron.* **6**, 1312 (2000).
2. R. Soref, *IEEE J. Sel. Top. Quantum Electron.* **12**, 1678 (2006).
3. M. Haurylau, G. Q. Chen, H. Chen, J. D. Zhang, N. A. Nelson, D. H. Albonese, E. G. Friedman, and P. M. Fauchet, *IEEE J. Sel. Top. Quantum Electron.* **12**, 1699 (2006).
4. G. S. Oehrlein, *Mater. Sci. Eng., B* **4**, 441 (1989).
5. M. Borselli, T. J. Johnson, and O. Painter, *Opt. Express* **13**, 1515 (2005).
6. M. Soltani, Q. Li, S. Yegnanarayanan, and A. Adibi, *Opt. Express* **15**, 17305 (2007).
7. V. R. Almeida and M. Lipson, *Opt. Lett.* **29**, 2387 (2004).
8. P. E. Barclay, K. Srinivasan, and O. Painter, *Opt. Express* **13**, 801 (2005).
9. L. He, Y. F. Xiao, C. Dong, J. Zhu, V. Gaddam, and L. Yang, *Appl. Phys. Lett.* **93**, 201102 (2008).
10. C. Schmidt, A. Chipouline, T. Kasebier, E. B. Kley, A. Tunnermann, and T. Pertsch, *Opt. Lett.* **35**, 3351 (2010).
11. I. Grudin, H. Lee, T. Chen, and K. Vahala, *Opt. Express* **19**, 7365 (2011).
12. M. Soltani, "Novel integrated silicon nanophotonic structures using ultra-high Q resonators," Ph.D. thesis (Georgia Institute of Technology, 2009).
13. J. Cardenas, C. B. Poitras, J. T. Robinson, K. Preston, L. Chen, and M. Lipson, *Opt. Express* **17**, 4752 (2009).
14. L. W. Luo, G. S. Wiederhecker, J. Cardenas, C. Poitras, and M. Lipson, *Opt. Express* **19**, 6284 (2011).
15. V. R. Almeida, C. A. Barrios, R. R. Panepucci, and M. Lipson, *Nature* **431**, 1081 (2004).
16. J. V. Campenhout, W. M. J. Green, X. Liu, S. Assefa, R. M. Osgood, and Y. A. Vlasov, *Opt. Lett.* **34**, 1534 (2009).